

Supporting Information

Iron Oxide Photoanode with Hierarchical Nanostructure for Efficient Water Oxidation

Tae-Youl Yang,^{†,‡,§} Ho-Young Kang,^{†,§} Kyoungsuk Jin,[†] Sangbaek Park,^{†,‡} Ji-Hoon Lee,[†]
Uk Sim,[†] Hui-Yun Jeong,[†] Young-Chang Joo,^{†,‡,*} and Ki Tae Nam^{†,‡,*}

[†] Department of Materials Science & Engineering, Seoul National University, 1 Gwanak-ro, Gwanak-gu,
151-744 Seoul, Republic of Korea

[‡] Research Institute of Advanced Materials (RIAM), Seoul National University, 1 Gwanak-ro, Gwanak-
gu, 151-742 Seoul, Republic of Korea

E-mail: nkitae@snu.ac.kr

E-mail: ycjoo@snu.ac.kr

[§] These authors contributed equally to this work.

1. Hydrothermal synthesis process

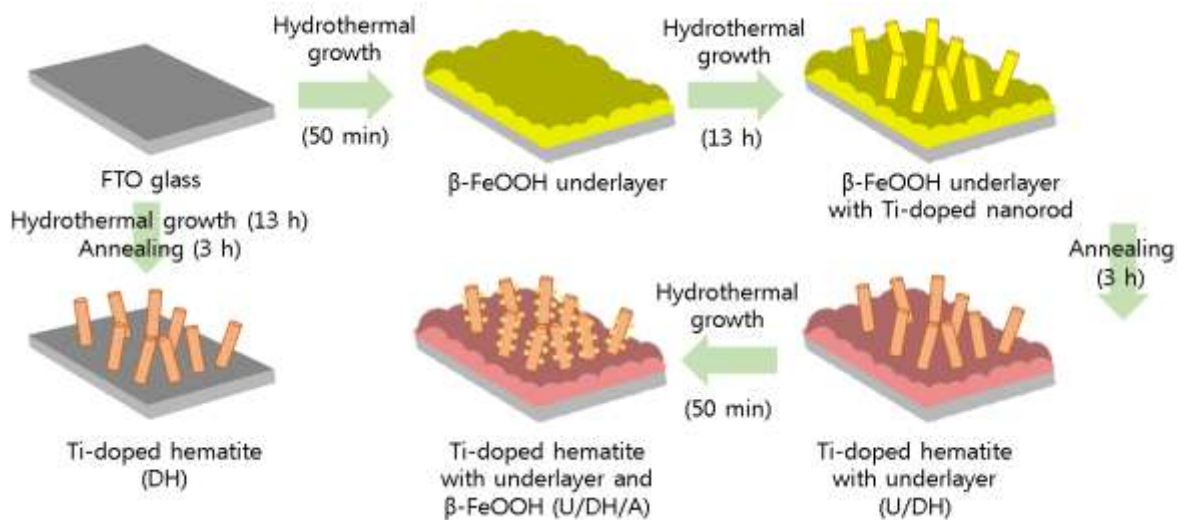


Figure S1. The procedure to fabricate a nanostructured hematite photoanode using hydrothermal synthesis.

Figure S1 summarizes the steps used to fabricate the hematite photoanode. β -FeOOH is formed by hydrothermal synthesis using an aqueous solution containing 0.15 M FeCl_3 and 1 M NaNO_3 . Two FTO substrates were immersed into the solution in an autoclave composed of a stainless steel body and a Teflon inner chamber with 70-ml-volume. Then, several autoclaves were heated at 95 °C. To convert β -FeOOH into hematite, an additional annealing at 550 °C is needed.

2. Characterization of the hematite photoanode

A. Phase change of the nanorods prepared by hydrothermal synthesis: X-ray diffraction

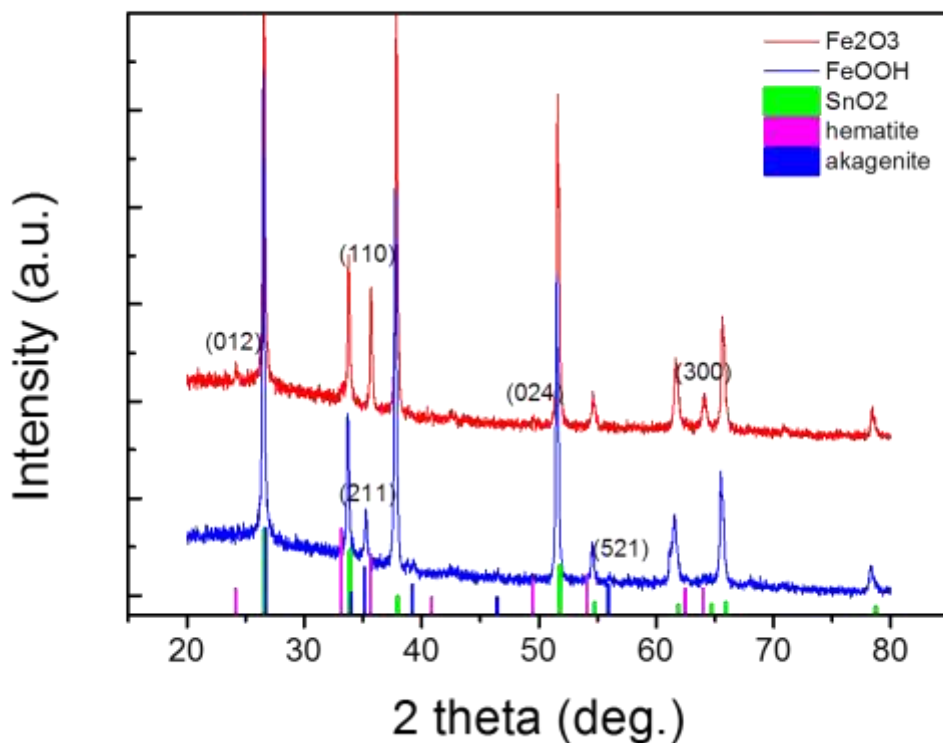


Figure S2. XRD patterns of β -FeOOH and hematite synthesized using hydrothermal method. The black line indicates hematite that has a preferred orientation of (110), and the red line indicates β -FeOOH that has a (211) orientation. The green dots indicate peaks from the FTO substrate.

Figure S2 presents the XRD patterns of β -FeOOH and hematite grown on FTO substrates by hydrothermal synthesis. β -FeOOH shows a preferred orientation of (211), and hematite shows a preferred orientation of (110), which has advantages in electron conduction.

B. Chemical state of elements in Ti-doped hematite

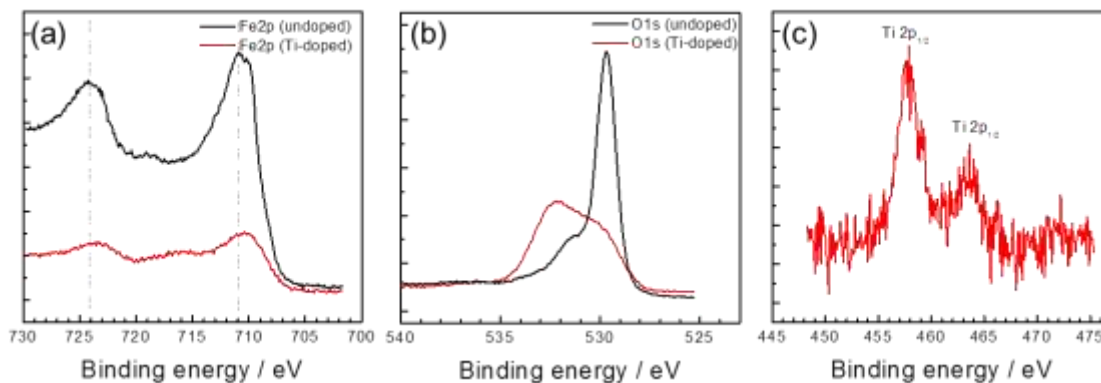


Figure S3. XPS spectra for (a) Fe2p, (b) Ti2p, and (b) O1s cores for undoped (black lines) and Ti-doped (red lines) hematite.

The Ti2p_{2/3} and Ti2p_{1/2} peaks for Ti-O bonds were detected at a binding energy of 457.7 eV and 463.6 eV, respectively. The excessive electrons from Ti ions shift the Fe2p peaks toward to lower binding energy (Figure 2a). In the spectra for O1s, the positive shift of peaks also indicates that oxygen forms bonding with the other element, Ti, which has lower electronegativity than Fe. These results indicate that Ti-ions well incorporated in hematite lattice in the oxide form.

C. Absorbance: UV-Vis spectroscopy

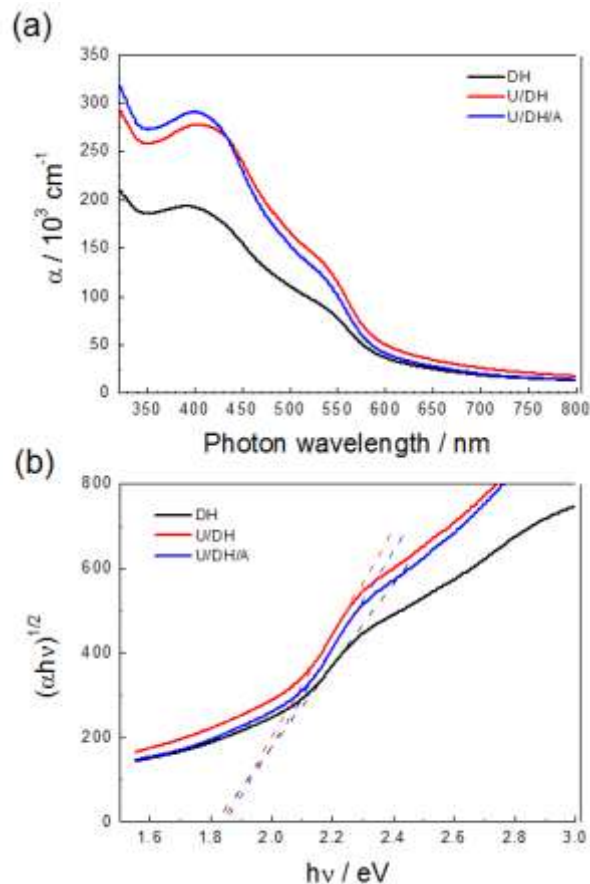


Figure S4. Absorbance of DH, U/DH, and U/DH/A from UV-visible spectroscopy.

To compare the light absorption of DH, U/DH, and U/DH/A, UV-visible spectroscopy was performed. As shown in Figure S3a, U/DH and U/DH/A have similar absorption coefficients and greater absorption than DH. Therefore, the undoped hematite underlayer contributes to light absorption, whereas the β -FeOOH does not. Figure S3b indicates that the band gap energies of DH, U/DH, and U/DH/A are all the same, which is inferred from the intercept between the tangent line of the curve and the x-axis.

D. Morphology: Scanning electron microscope

For synthesizing the nanostructured hematite photoanode, β -FeOOH branches are synthesized on Ti-doped hematite that was subjected to heat treatment at 550 °C. β -FeOOH was also synthesized on Ti-doped nanorods that were not annealed. Those β -FeOOH did not form branches on the nanorods, as shown in Figure S4a and S4b, but only caused an increase in the thicknesses of the nanorod films, whereas the β -FeOOH synthesized on hematite forms nano-branches, as shown in Figure S5.

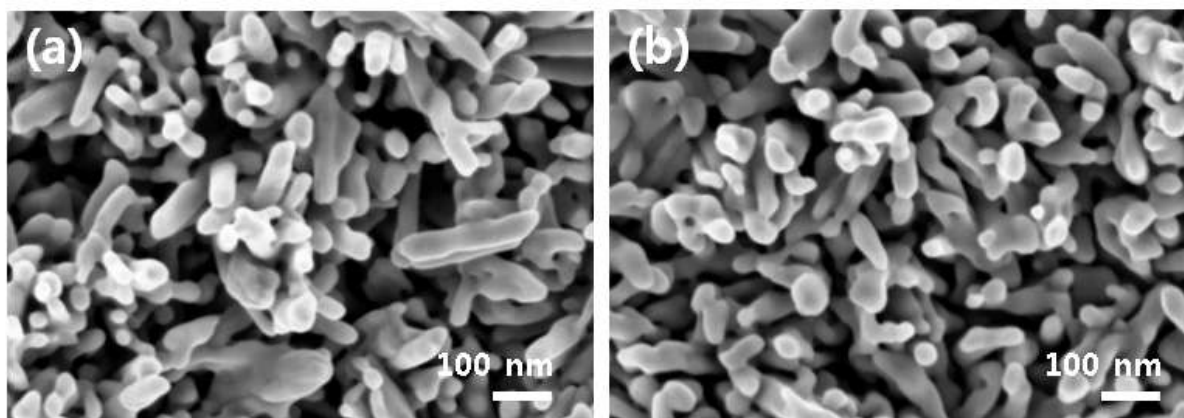


Figure S5. SEM images of hydrothermally synthesized (a) Ti-doped hematite nanorod, and (b) β -FeOOH grown on (a) before annealed at 550 °C

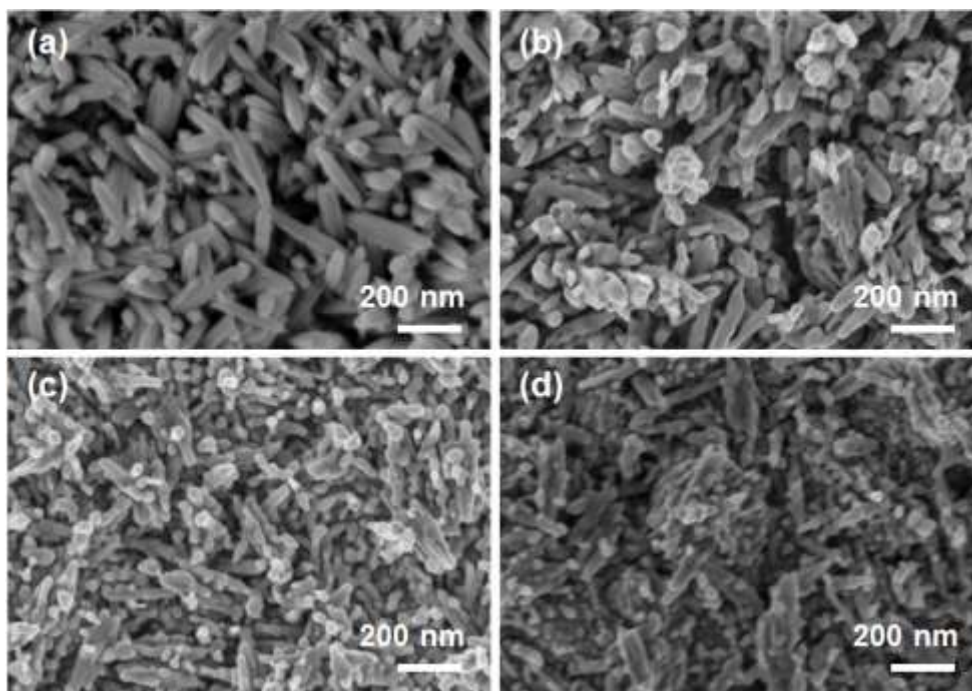


Figure S6. Morphology of Ti-doped hematite nanorod array depending on the concentration of the Ti-dopants. (a) undoped hematite, (b) 1% Ti-doped hematite, (c) 5% Ti-doped hematite, (d) 10% Ti-doped hematite.

The morphological dependence on the Ti-dopant concentration was observed using SEM. As shown in Figure S6, Ti-doping induces a less-ordered structure of hematite nanorods, and when the doping level increases, the thicknesses of the nanorods decreases and the nanorods are less ordered.

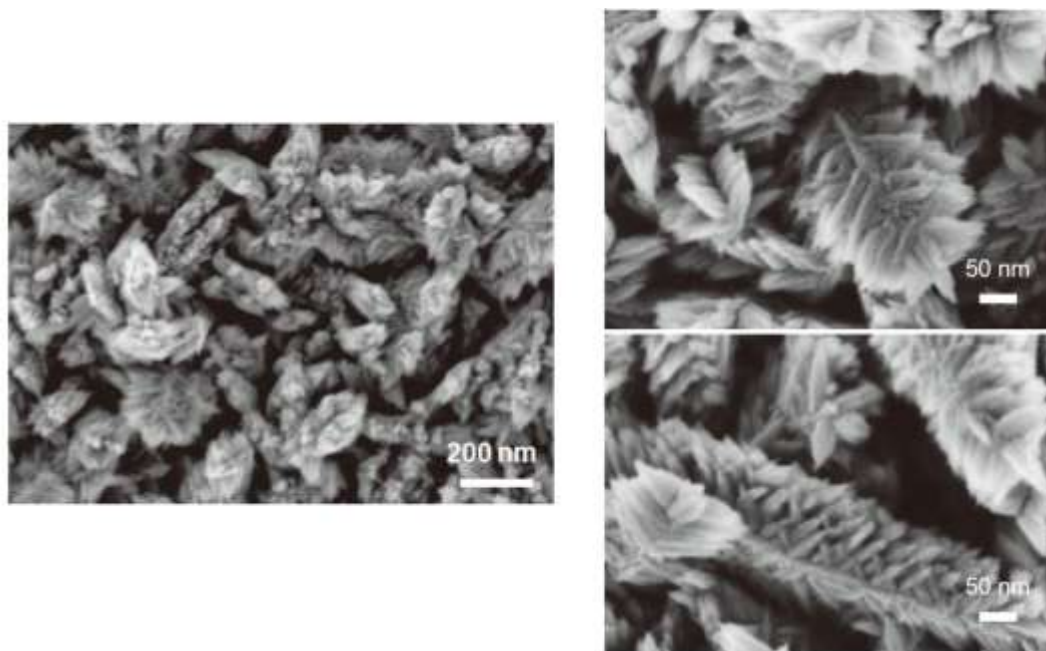


Figure S7. SEM images of hydrothermally synthesized hematite nanorods after additional hydrothermal synthesis for 50 min.

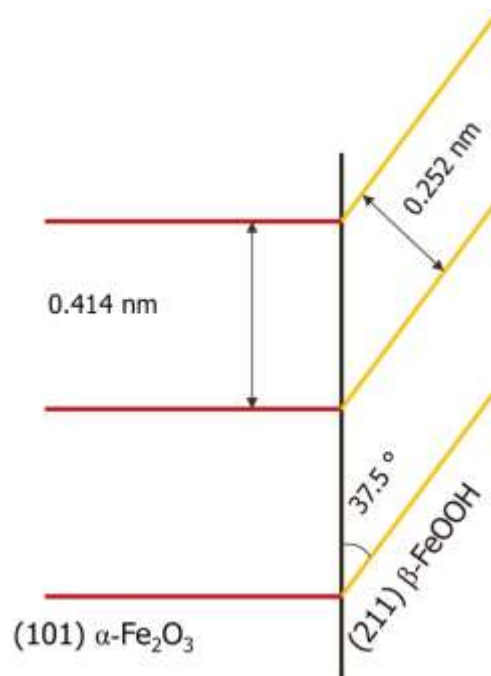


Figure S8. Schematic picture of the lattice matching between hematite and $\beta\text{-FeOOH}$. (101) planes of hematite (red line) and (211) planes of $\beta\text{-FeOOH}$ (yellow line) are indicated.

E. Electrochemical analysis

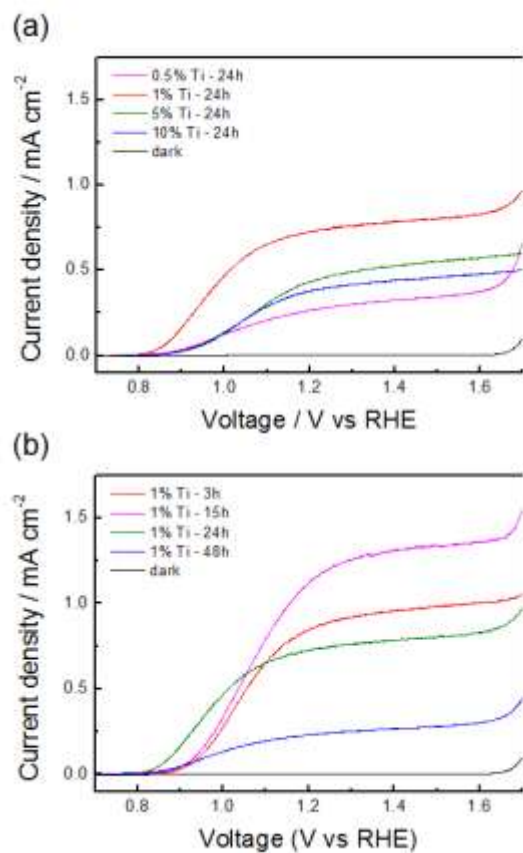


Figure S9. *J-E* curves for Ti-doped hematite when (a) the concentration of Ti-dopant is varied from 0 - 10 at. %, and (b) the synthetic time for fabricating 1 at. % Ti-doped hematite is varied from 3 - 48 h.

The effects of the synthesis time and Ti dopant concentration are plotted in Figure S8. The effect of the Ti dopant concentration, which was varied from 0 - 10 at. %, is plotted in Figure S8a and indicates that there is an optimum doping concentration of 1 at. %. Up to a concentration of 1 at. %, the photocurrent increases with increasing dopant concentration, but above 1 at. %, the opposite occurs. Because too little dopant cannot provide hematite with sufficient electron conductivity and because too much dopant causes lower electron conductivity due to the scattering effect by ionized donors, there is an optimum doping level that provides hematite with maximum electron conductivity. Figure S8b shows the effect of the synthesis time, which was

varied from 3 h - 48 h and indicates that the photocurrent is increased up to a synthesis time of 15 h but then starts to decrease as the synthesis time increases. Because hematite has an indirect band gap, hematite requires a thickness of hundreds of nanometers to effectively absorb photons, whereas the increase of the thickness induces an increase in the resistance to electrons moving to the FTO substrate. Therefore, an optimum thickness of hematite exists and is obtained at approximately 15 h in our system.

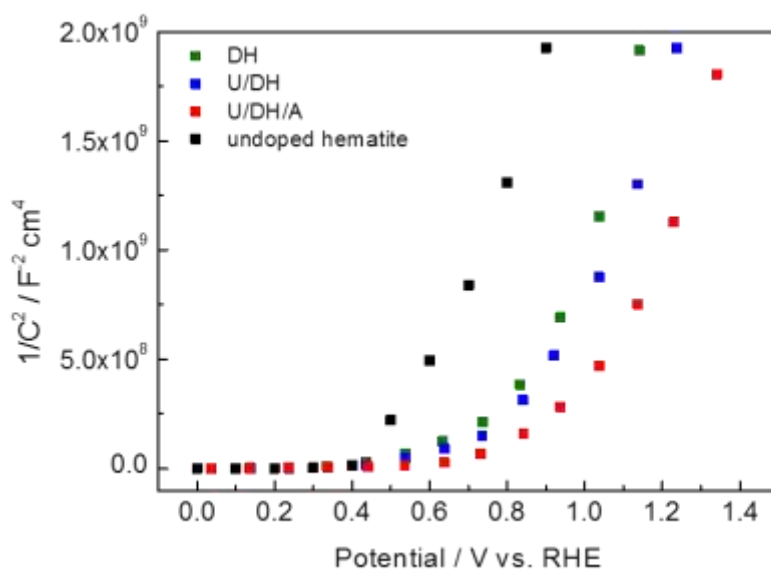


Figure S10. Mott-Schottky plot of DH, U/DH, U/DH/A, and undoped hematite nanorods measured under dark condition.

Table S1. Donor density and flat band potential calculated from Mott-Schottky plot.

	Undoped hematite	DH	U/DH	U/DH/A
Donor density (cm ⁻²)	5.50×10^{20}	2.06×10^{21}	2.55×10^{21}	1.62×10^{21}
Flatband potential (V vs. RHE)	0.42	0.44	0.46	0.65

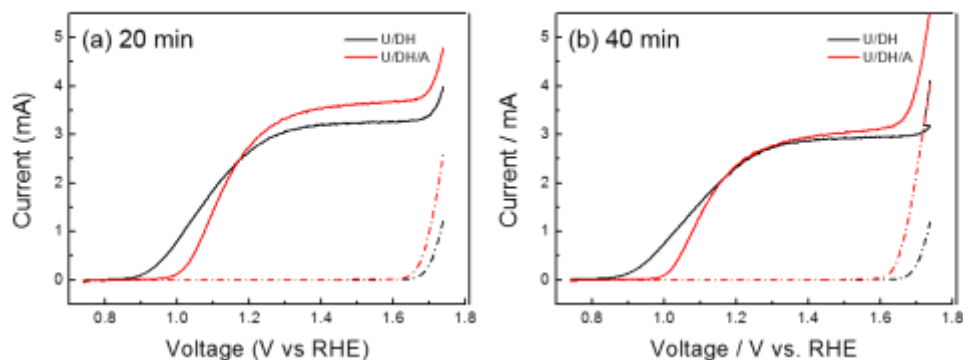


Figure S11. Comparison of J - E curves for U/DH/A to U/DH under illumination when β -FeOOH is grown (a) for 10 min and (b) for 40 min.

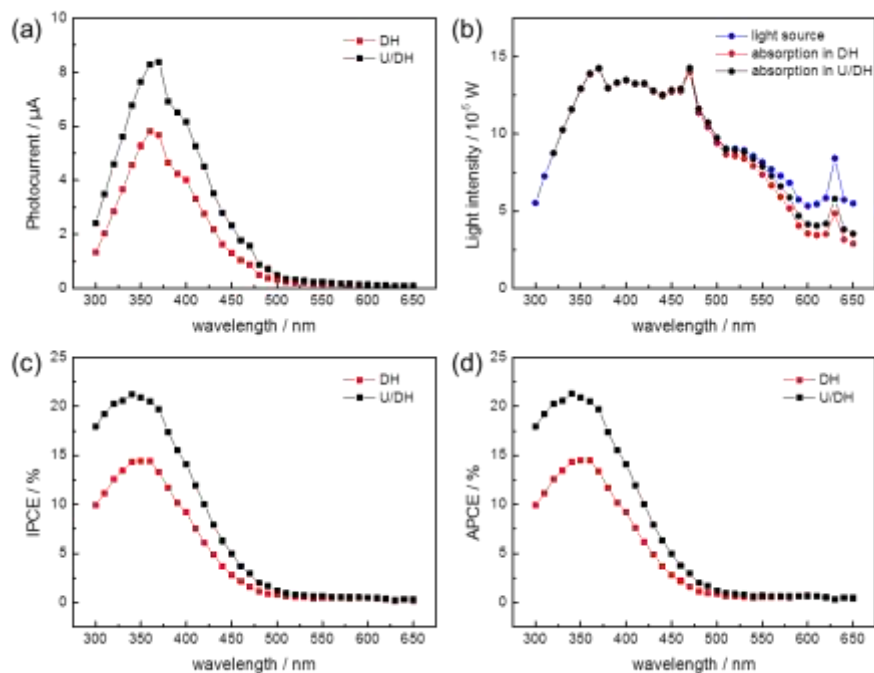


Figure S12. Spectral response of DH and U/DH electrodes. (a) solar photocurrent spectra, (b) absorbed light intensity spectra, (c) Incident photon to current conversion efficiency, (d) absorbed photon to current efficiency (quantum yield)

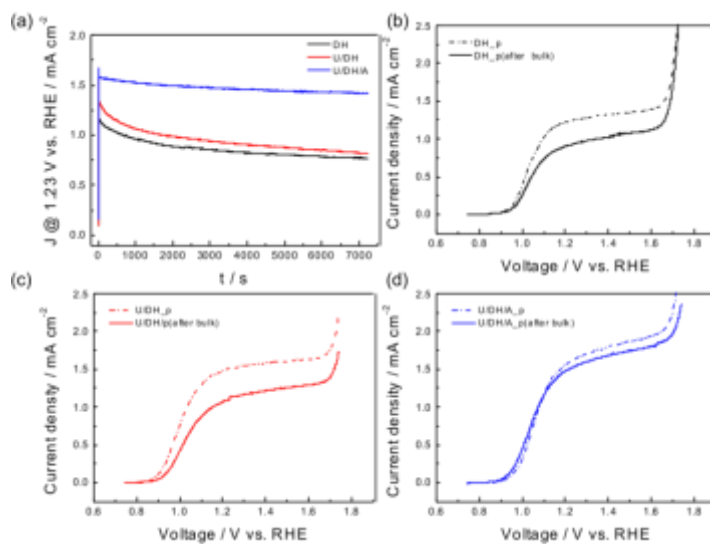


Figure S13. Photoelectrochemical stability of hematite photoanodes. (a) Changes in photocurrent at 1.23 V vs. RHE during chronoamperometry test. J - V curves before and after the chronoamperometry test are compared for (a) DH, (b) U/DH, and (c) U/DH/A photoanodes.